Int. J. Solids Structures Vol. 20, No. 11/12, pp. 1009–1019, 1984
Printed in the U.S.A.

0020–7683/84 $3.00 + .00
Pergamon Press Ltd.

NONLINEAR BENDING OF RECTANGULAR ORTHOTROPIC PLATE WITH TWO FREE EDGES AND THE OTHER EDGES HAVING NONUNIFORM ROTATIONAL FLEXIBILITY

CANGRU JIANG† AND CHUEN-YAUN CHIA
Department of Civil Engineering, University of Calgary, Calgary, Alberta, Canada T2N 1N4

(*Received* 25 *July* 1983; *in revised form* 9 *January* 1984)

Abstract—this paper presents a series solution to von Kármán nonlinear equations of a rectilinearly orthotropic rectangular plate under the combined action of lateral load and in-plane tension with the titled edge restraints. In the formulation the edge moments are replaced by an equivalent pressure near the edges. Using generalized double Fourier series for the deflection and stress function, governing equations are reduced to an infinite set of algebraic equations for coefficients in these series. Numerical results for deflections, bending moments and in-plane forces are graphically presented for various values of aspect ratio and material properties and for different edge conditions.

NOTATION

A_{mn} Fourier constants given by (29)
a, b length and width of plate, respectively
a_p, b_p Fourier constants given by (25) and (27), respectively
C_m, D_m constant coefficients (m = 1, 2, 3, . . .) given in (13)
c_i material constants (i = 1, 2, 3, 4, 5) defined in (3) and (13)
E_1, E_2 principal Young's moduli
F nondimensional stress function defined in (3)
F_{mn} Fourier constants given by (30) and (32)
G_{12} shear modulus
G_i^{mn} constants (i = 1, 2, . . . , 5) defined in (31) and (33)
H_i norm of $X_m(\zeta)$ given by (14)
h thickness of plate
$K_i^{pq}, \bar{K}_i^{pq}$ constants (i = 1, 2, . . . , 8) defined in (26), (31) and (33)
$k_1)\zeta), k_2(\zeta)$ rotational edge-restraint coefficients defined by (8a) and (9a)
$L_i^{pq}, \bar{L}_i^{pq}$ constants (i = 1, 2, . . . , 8) defined in (28), (31) and (33)
M_x, M_y, M_{xy} bending and twisting moments per unit length
$M_\zeta, M_\eta, M_{\zeta\eta}$ nondimensional bending and twisting moments defined in (5)
$M_{0\eta}, M_{1\eta}$ nondimensional edge moments given by (18)
N_x, N_y, N_{xy} in-plane forces per unit length
$N_\zeta, N_\eta, N_{\zeta\eta}$ nondimensional in-plane forces defined in (5)
P nondimensional in-plane tension ($= pb^2/E_2h^3$)
p in-plane tension per unit length
Q nondimensional load intensity defined in (3)
q laterally distributed load per unit area
Q_e lateral pressure equivalent to nondimensional edge moments given by (17) or (19)
Q_{mn} Fourier constants given by (22)
Q_x, Q_y shearing forces per unit length
Q_ζ, Q_η nondimensional shearing forces defined in (5)
Q^* sum of Q and Q_e
Q^*_{mn} Fourier constants given by (24)
R_m, S_n orthogonal beam functions defined in (12)
V_x transverse edge force per unit length
V_ζ nondimensional transverse edge force defined in (5)
W nondimensional deflection defined in (3)
W_{mn} Fourier constants given by (30) and (32)
w deflection
X_m orthogonal beam functions defined in (12)
x, y, z rectangular coordinates
$\alpha_m, \beta_m, \gamma_m$ constant coefficients (m = 1, 2, 3, . . .) given by (15), (16) and (13) respectively
δ_1, δ_2 coefficients given in Table 3
ζ, η nondimensional coordinates defined in (3)

† On leave from Wuhan Institute of Building Materials, Wuhan, Hubei, China.

λ aspect ratio of plate
ν_{12}, ν_{21} Poisson's ratios
ψ stress function
$(\ )_{,i}$ partial differentiation with respect to i coordinate
$(\ )'$ ordinary differentiation with respect to the corresponding coordinate

INTRODUCTION

The geometrically nonlinear behaviour of elastic plates has been studied by a great number of investigators [1]. Most of the existing solutions, however, are restricted to simple boundary conditions.

In reality a structural plate is generally restrained elastically and nonuniformly against rotation along its edges. Employing the Ritz method Stippes [2] has studied the large-deflection problem of a rectangular plate with two opposite edges simply supported and the other edges simply supported, elastically supported or free from forces and moments. Numerical results are reported only for a simply supported plate along its four edges. In the case of circular plates with mixed boundary conditions static and dynamic problems have been considered by Ramachandran [3], Nowinski [4] and Banerjee [5] using Berger's hypothesis. Nonlinear asymmetric bending of annular plates has been discussed by Alzheimer and Davis [6] and Tielking [7] using the von Kármán plate theory. In the linear case bending of a rectangular plate with one or more free edges has been treated by Huang and Conway [8] and Fletcher and Thorne [9] and can be also found in the text by Timoshenko and Woinowsky-Krieger [10] or elsewhere. Stability and vibration of thin plates have received considerable attention, especially in recent years. A review of the literature is referred to the previous work [11–14].

This study is analytically concerned with nonlinear bending of an orthotropic rectangular plate with two opposite edges free from in-plane forces and bending moments and the other edges having nonuniform elastic constraints against rotation. The plate is subjected to lateral load and uniaxial in-plane tension. Using different generalized double Fourier series for the deflection and stress function, the required boundary conditions are fulfilled and the von Kármán nonlinear equations of the plate are reduced to an infinite set of algebraic equations for Fourier constants in these series. Convergent solutions can be determined to any desired degree of accuracy by successive truncation of this set of equations.

GOVERNING EQUATIONS

Consider a thin rectilinearly orthotropic rectangular elastic plate of length a in the x direction, width b in the y direction and thickness h in the z direction. The midsurface of the undeformed plate contains the x, y axes. The origin of the coordinate system is taken at one of the plate corners. The material axes of symmetry are assumed to be parallel to these axes. The von Kármán nonlinear equations of the plate under laterally distributed load of intensity $q(x\ y)$ are given by eqns (5.24) and (5.25) of Ref. [1]. If the deflection and stress function are represented by w and ψ respectively, these equations may be written in the nondimensional form as:

$$c_1 W_{,\zeta\zeta\zeta\zeta} + 2\lambda^2 c_2 W_{,\zeta\zeta\eta\eta} + \lambda^4 W_{,\eta\eta\eta\eta} = \lambda^4 c_3 Q + \lambda^2 c_3 (W_{,\zeta\zeta} F_{,\eta\eta} + W_{,\eta\eta} F_{,\zeta\zeta} - 2W_{,\zeta\eta} F_{,\zeta\eta}) \tag{1}$$

$$c_1 F_{,\zeta\zeta\zeta\zeta} + 2\lambda^2 c_4 F_{,\zeta\zeta\eta\eta} + \lambda^4 F_{,\eta\eta\eta\eta} = c_1 \lambda^2 (W_{,\zeta\eta}^2 - W_{,\zeta\zeta} W_{,\eta\eta}) \tag{2}$$

in which a comma denotes partial differentiation with respect to the corresponding coordinates and in which

$$\zeta = x/a, \quad \eta = y/b, \quad \lambda = a/b, \quad F = \psi/E_2 h^3, \quad W = w/h, \quad Q = qb^4/E_2 h^4$$
$$c_1 = E_1/E_2, \quad c_2 = \nu_{12} + c_3 G_{12}/6E_2, \quad c_3 = 12(1 - \nu_{12}\nu_{21}), \tag{3}$$
$$c_4 = 0.5(E_1/G_{12} - 2\nu_{12})$$

In eqns (3) E_2 and E_1 are principal Young's moduli, ν_{12} and ν_{21} are Poisson's ratios, and G_{12} is the shear modulus.

The nondimensional bending moments, in-plane forces, transverse shear forces and vertical edge force are related to the nondimensional deflection and stress function, respectively, by

$$\begin{aligned}
M_\zeta &= -(c_1 W_{,\zeta\zeta} + \lambda^2 \nu_{12} W_{,\eta\eta})/c_3\lambda^2 \\
M_\eta &= -(\nu_{12} W_{,\zeta\zeta} + \lambda^2 W_{,\eta\eta})/c_3\lambda^2 \\
M_{\zeta\eta} &= -(G_{12}/6\lambda E_2) W_{,\zeta\eta} \\
N_\zeta &= F_{,\eta\eta} \\
N_\eta &= F_{,\zeta\zeta}/\lambda^2 \\
N_{\zeta\eta} &= -F_{,\zeta\eta}/\lambda \\
Q_\zeta &= -(c_1/c_3\lambda^3) W_{,\zeta\zeta\zeta} - (\nu_{12}/c_3\lambda + G_{12}/6E_2\lambda) W_{,\zeta\eta\eta} \\
Q_\eta &= -(1/c_3) W_{,\eta\eta\eta} - (\nu_{12}/c_3\lambda^2 + c_3 G_{12}/72E_2\lambda^2) W_{,\zeta\zeta\eta} \\
V_\zeta &= Q_\zeta + M_{\zeta\eta,\eta}
\end{aligned} \tag{4}$$

where

$$\begin{aligned}
(M_\zeta, M_\eta, M_{\zeta\eta}) &= (M_x, M_y, M_{xy}) b^2/E_2 h^4 \\
(N_\zeta, N_\eta, N_{\zeta\eta}) &= (N_x, N_y, N_{xy}) b^2/E_2 H^3 \\
V_\zeta &= V_x b^3/E_2 h^4 \\
(Q_\zeta, Q_\eta) &= (Q_x, Q_y) b^3/E_2 h^4.
\end{aligned} \tag{5}$$

In eqns (5) M_i, N_i, Q_i and V_x are bending moments, in-plane forces, transverse shear force and transverse edge force per unit length, respectively.

In addition to the lateral load the plate edges, $y = 0$, b, are also subjected to in-plane tension per unit length, p, in the y direction. For the out-of-plane boundary conditions these edges are assumed to be elastically restrained against rotation. The rotational stiffnesses are allowed to vary along these edges. The other two edges are

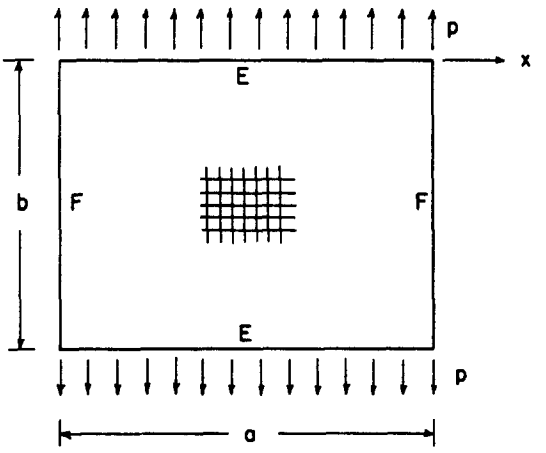

Fig. 1. Geometry, elastic directions, boundary conditions and in-plane tension of orthotropic rectangular plate (E = nonuniformly elastically restrained edge against rotation, F = free edge).

free from forces and bending moments. Such a plate is shown in Fig. 1. The appropriate boundary conditions are also written in the nondimensional form as

$$M_\zeta = 0, \quad V_\zeta = 0, \quad N_\zeta = 0, \quad N_{\zeta\eta} = 0 \qquad \text{at } \zeta = 0 \qquad \text{(6a–d)}$$

$$M_\zeta = 0, \quad V_\zeta = 0, \quad N_\zeta = 0, \quad N_{\zeta\eta} = 0 \qquad \text{at } \zeta = 1 \qquad \text{(7a–d)}$$

$$M_\eta = k_1(\zeta)W_{,\eta}, \quad W = 0, \quad N_\eta = P, \quad N_{\zeta\eta} = 0 \qquad \text{at } \eta = 0 \qquad \text{(8a–d)}$$

$$M_\eta = -k_2(\zeta)W_{,\eta}, \quad W = 0, \quad N_\eta = P, \quad N_{\zeta\eta} = 0 \qquad \text{at } \eta = 1 \qquad \text{(9a–d)}$$

in which k_1 and k_2 are rotational edge-restraint coefficients, functions of ζ, and P is the nondimensional in-plane tension given by pb^2/E_2h^3.

The system of eqns (1) and (2) are thus to be solved in conjunction with boundary conditions (6)–(9).

METHOD OF SOLUTION

A solution of eqns (1) and (2) is sought in the form of generalized double Fourier series:

$$W = \sum_{m,n=1}^{\infty}\sum W_{mn}X_m(\zeta)\sin n\pi\eta \tag{10}$$

$$F = P\zeta^2/2 + \sum_{m,n=1}^{\infty}\sum F_{mn}R_m(\zeta)S_n(\eta) \tag{11}$$

in which $X_m(\zeta)$, $R_m(\zeta)$ and $S_n(\eta)$ are orthogonal beam functions given by:

$$\begin{aligned} X_m(\zeta) &= \cosh\alpha_m\zeta + \cos\alpha_m\zeta + C_m\sinh\alpha_m\zeta + D_m\sin\alpha_m\zeta \\ R_m(\zeta) &= \cosh\beta_m\zeta - \cos\beta_m\zeta - \gamma_m(\sinh\beta_m\zeta - \sin\beta_m\zeta) \\ S_n(\eta) &= \cosh\beta_n\eta - \cos\beta_n\eta - \gamma_n(\sinh\beta_n\eta - \sin\beta_n\eta) \end{aligned} \tag{12}$$

where

$$\begin{aligned} C_m &= \frac{\cos\alpha_m - \cosh\alpha_m}{\sinh\alpha_m - \sin\alpha_m(\alpha_m^2 + c_5n^2\pi^2)/(\alpha_m^2 - c_5n^2\pi^2)} \\ D_m &= \frac{\cos\alpha_m - \cosh\alpha_m}{\sinh\alpha_m(\alpha_m^2 - c_5n^2\pi^2)/(\alpha_m^2 + c_5n^2\pi^2) - \sin\alpha_m} \\ c_5 &= \lambda^2(\gamma_m/c_1 + c_3G_{12}/3E_1) \\ \gamma_i &= \frac{\sinh\beta_i + \sin\beta_i}{\cosh\beta_i - \cos\beta_i}. \end{aligned} \tag{13}$$

The orthogonal functions (12) possess the following properties:

$$\begin{aligned} \int_0^1 X_i(\zeta)X_j(\zeta)\,d\zeta &= \begin{cases} 0, & i \neq j \\ H_i, & i = j \end{cases} \\ \int_0^1 R_i(\zeta)R_j(\zeta)\,d\zeta &= \begin{cases} 0, & i \neq j \\ 1, & i = j \end{cases} \\ \int_0^1 S_i(\eta)S_j(\eta)\,d\eta &= \begin{cases} 0, & i \neq j \\ 1, & i = j \end{cases} \end{aligned} \tag{14}$$

Where H_i is the norm of $X_i(\zeta)$. The expression for H_i is lengthy and hence not presented herein.

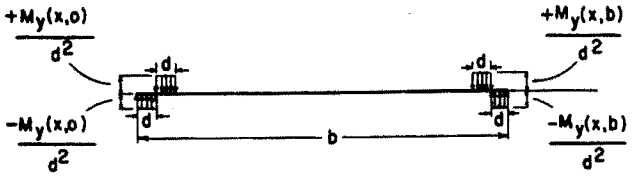

Fig. 2. Equivalent pressure distribution ($d \to 0$) for edge moments.

It may be observed that expression (10) for W satisfies the boundary conditions (6a,b) (7a,b), (8b) and (9b) if α_m are the roots of the transcendental equation

$$\frac{1}{2}\left(\frac{\alpha_m^2 - c_5 n^2\pi^2}{\alpha_m^2 + c_5 n^2\pi^2} - \frac{\alpha_m^2 + c_5 n^2\pi^2}{\alpha_m^2 - c_5 n^2\pi^2}\right) \sinh \alpha_m \sin \alpha_m + \cosh \alpha_m \cos \alpha_m - 1 = 0 \quad (15)$$

and that the boundary conditions (c) and (d) of eqns (6)–(9) are satisfied if β_i are the roots of the equation

$$\cosh \beta_i \cos \beta_i - 1 = 0. \quad (16)$$

Now only boundary conditions (8a) and (9a) are to be fulfilled.

In this analysis the bending moments along the edges $\eta = 0, 1$ as required in boundary conditions (8a) and (9a) are replaced by an equivalent lateral pressure, denoted by Q_e, near these edges as shown in Fig. 2. If this pressure is represented by a Fourier series, we find, as d approaches to zero,

$$Q_e = 2\pi \sum_{s=1}^{\infty} [M_{0\eta} - (-1)^s M_{1\eta}] s \sin s\pi\eta \quad (17)$$

in which $M_{0\eta}$ and $M_{1\eta}$ are bending moments at $\eta = 0$ and $\eta = 1$, respectively. They are also expanded into series in terms of orthogonal functions as:

$$M_{0\eta} = \frac{1}{2\pi} \sum_{p=1}^{\infty} a_p X_p(\zeta) \quad (18a)$$

$$M_{1\eta} = \frac{1}{2\pi} \sum_{p=1}^{\infty} b_p X_p(\zeta) \quad (18b)$$

where Fourier constants a_p and b_p are to be determined later. Introducing expressions (18) in (17) we obtain:

$$Q_e = \sum_{m,n=1}^{\infty}\sum A_{mn} X_m(\zeta) \sin n\pi\eta \quad (19)$$

where

$$A_{mn} = n[a_m - (-1)^n b_m]. \quad (20)$$

The applied lateral load $Q(\zeta, \eta)$ can be expanded into a generalized Fourier series as:

$$Q(\zeta, \eta) = \sum_{m,n=1}^{\infty}\sum Q_{mn} X_m(\zeta) \sin n\pi\eta \quad (21)$$

where

$$Q_{mn} = \frac{1}{2H_m} \int_0^1 \int_0^1 Q(\zeta, \eta) X_m(\zeta) \sin n\pi\eta \, d\zeta \, d\eta. \tag{22}$$

Then the loading term in eqn (1), which is the sum of $Q(\zeta, \eta)$ and $Q_c(\zeta, \eta)$, can be written as:

$$Q^*(\zeta, \eta) = \sum_{m,n=1}^{\infty} \sum Q^*_{mn} X_m(\zeta) \sin n\pi\eta \tag{23}$$

where

$$Q^*_{mn} = A_{mn} + Q_{mn}. \tag{24}$$

Inserting expressions (10) and (18a) into the boundary condition (8a), multiplying both sides of the resulting equation by $X_p(\zeta)$ and integrating with respect to ζ over the interval (0, 1), the boundary condition transforms to

$$a_p = \frac{2\pi^2}{H_p} \sum_{m,n=1}^{\infty} \sum n W_{mn} K_1^{pm} \tag{25}$$

where

$$K_1^{pm} = \int_0^1 k_1(\zeta) X_p(\zeta) X_m(\zeta) \, d\zeta. \tag{26}$$

Similarly, from boundary condition (9a) and expressions (10) and (18b) the following is obtained:

$$b_p = \frac{2\pi^2}{H_p} \sum_{m,n=1}^{\infty} \sum (-1)^n n W_{mn} L_1^{pm} \tag{27}$$

where

$$L_1^{pm} = \int_0^1 k_2(\zeta) X_p(\zeta) X_m(\zeta) \, d\zeta. \tag{28}$$

Substitution of eqns (25) and (27) in expression (20) yields

$$A_{mn} = \frac{2\pi^2}{H_m} n \sum_{r,s=1}^{\infty} \sum s W_{rs} [K_1^{mr} - (-1)^{n+s} L_1^{mr}]. \tag{29}$$

It is observed that boundary conditions (8a) and (9a) for elastical edge restraints against rotation is fulfilled if the loading term in eqn (1) is replaced by expression (23) with A_{mn} given by eqn (29).

Inserting expressions (10) and (11) into compatibility equation (2), multiplying both sides of the resulting equation by $R_m(\zeta)S_n(\eta)$ and integrating with respect to ζ and η over the interval (0, 1) we obtain the following set of algebraic equations:

$$F_{mn} + G_1^{mn} \sum_{k,l=1}^{\infty} \sum F_{kl} K_2^{mk} L_2^{nl} = G_2^{mn} \sum_{k,r,l,s=1}^{\infty} \sum W_{kl} W_{rs} (l K_3^{mkr} L_3^{nls} + s K_4^{mkr} L_4^{nls})$$

$$m, n = 1, 2, 3, \ldots \tag{30}$$

where

$$G_1^{mn} = \frac{2c_4\lambda^2}{c_1\beta_m^4 + \lambda_4\beta_n^4}, \quad G_2^{mn} = \frac{c_1\lambda^2\pi^2}{c_1\beta_m^4 + \lambda^4\beta_n^4}$$

$$K_2^{mk} = \int_0^1 R_k''(\zeta)R_m(\zeta)\,d\zeta$$

$$L_2^{nl} = \int_0^1 S_l''(\eta)S_n(\eta)\,d\eta$$

$$K_3^{mkr} = \int_0^1 R_m(\zeta)X_k'(\zeta)X_r'(\zeta)\,d\zeta \tag{31}$$

$$L_3^{nls} = \int_0^1 S_n(\eta)\cos l\pi\eta\cos s\pi\eta\,d\eta$$

$$K_4^{mkr} = \int_0^1 R_m(\zeta)X_k''(\zeta)X_r(\zeta)\,d\zeta$$

$$L_4^{nls} = \int_0^1 S_n(\eta)\sin l\pi\eta\sin s\pi\eta\,d\eta.$$

In these expressions the primes denote differentiation with respect to the corresponding coordinate.

Similarly, eqn (1) is reduced to a set of algebraic equations as:

$$W_{mn} - G_3^{mn}\sum_{k=1}^{\infty} n^2 W_{kn}K_5^{mk} = G_4^{mn}Q_{mn} + G_5^{mn}\sum_{k,r,l,s=1}^{\infty}\sum W_{kl}F_{rs}$$
$$\times (K_6^{mkr}L_6^{nls} - \pi^2 l^2 K_7^{mkr}L_7^{nls} - 2\pi l K_8^{mkr}L_8^{nls}) \qquad m, n = 1, 2, 3, \ldots \tag{32}$$

where

$$G_3^{mn} = \frac{2\lambda^2\pi^2 c_2}{(c_1\alpha_m^4 + \lambda^4 n^4\pi^4 + \lambda^2\pi^2 n^2 c_3 P)H_m}$$

$$G_4^{mn} = \frac{\lambda^4 c_3}{(c_1\alpha_m^4 + \lambda^4\pi^4 n^4 + \lambda^2\pi^2 n^2 c_3 P)H_m}$$

$$G_5^{mn} = \frac{2\lambda^2 c_3}{(c_1\alpha_m^4 + \lambda^4\pi^4 n^4 + \lambda^2\pi^2 n^2 c_3 P)H_m}$$

$$K_5^{mk} = \int_0^1 X_m(\zeta)X_k''(\zeta)\,d\zeta$$

$$L_6^{nls} = \int_0^1 \sin n\pi\eta\sin l\pi\eta S_s''(\eta)\,d\eta \tag{33}$$

$$K_6^{mkr} = \int_0^1 X_m(\zeta)X_k''(\zeta)R_r(\zeta)\,d\zeta$$

$$L_7^{nls} = \int_0^1 \sin n\pi\eta\sin l\pi\eta S_s(\eta)\,d\eta$$

$$K_7^{mkr} = \int_0^1 X_m(\zeta)X_k(\zeta)R_r''(\zeta)\,d\zeta$$

$$L_8^{nls} = \int_0^1 \sin n\pi\eta\cos l\pi\eta S_s'(\eta)\,d\eta$$

$$K_8^{mkr} = \int_0^1 X_m(\zeta)X_k'(\zeta)R_r'(\zeta)\,d\zeta.$$

The infinite set of eqns (30) and (32) are to be truncated to obtain a solution for coefficients in series (10) and (11) for W and F. For various values of m, n these equations give the same number of terms taken in these series. Therefore, a solution with any desired degree of accuracy can be obtained for a set of given values in parameters E_1/E_2, ν_{12}, G_{12}/E_2, λ, k_1, k_2, P and Q.

NUMERICAL RESULTS AND DISCUSSION

Numerical results are presented for nonlinear behaviour of high-modulus composite rectangular plates. The elastic constants typical of these materials are given in Table 1. Table 2 presents the nondimensional central deflection, $W_0 = W(0.5, 0.5)$, of a square plate with different loading and boundary conditions obtained from nine terms and sixteen terms in each of the truncated series for F and W. The nondimensional in-plane tensile force used in calculation is shown. It can be seen from this table that these series converge considerably rapidly. A comparison of small deflections and bending moments at the center of an isotropic plate is shown in Table 3. A good agreement is noticed between two sets of values.

Figure 3 shows the load-deflection relations of a graphite-epoxy (GR) rectangular plate under uniform lateral load q_o and of isotropic and glass-epoxy (GL) rectangular plates under the combined action of uniform lateral load and in-plane tension.† The edge conditions of these plates are free in the x direction and simply supported in the y direction. The central deflection of these plates decreases with an increase in the aspect ratio. This arises from the fact that the distance from the plate center to the free edges increases with this ratio. The effect of the uniform rotational edge restraint

Table 1. Numerical values of elastic constants

Material	E_2/E_1	G_{12}/E_1	ν_{12}
Glass-epoxy	3.0	0.6	0.25
Graphite-epoxy	40.0	0.5	0.25

Table 2. Comparison of nine-term and sixteen-term solutions for central deflections W_0 of square plate with two opposite free edges and two simply supported edges

Q	GR, P = 0		GL, P = 10	
	9 terms	16 terms	9 terms	16 terms
100	1.4225	1.4234	1.0607	1.0624
200	2.0012	2.0075	1.5025	1.5049
300	2.3943	2.4021	1.8233	1.8276
600	3.4037	3.4215	2.2035	2.2144

Table 3. Comparison of small central deflection and moment for isotropic plate with two opposite free edges and two simply supported edges ($\nu = 0.3$, $P = 0$)

λ	$W_o = \delta_1 Q$		$M_\eta = \delta_2 Q$	
	δ_1		δ_2	
	Present	Ref. 10	Present	Ref. 10
0.5	0.1492	0.1504	0.1228	0.1235
1.0	0.1421	0.1429	0.1218	0.1225
2.0	0.1380	0.1408	0.1226	0.1235
∞	0.1395	0.1422	0.1230	0.1250

† Numerical calculations were carried out by a Multics computer. The maximum time for a solution of any special problem presented herein is less than 1600 sec.

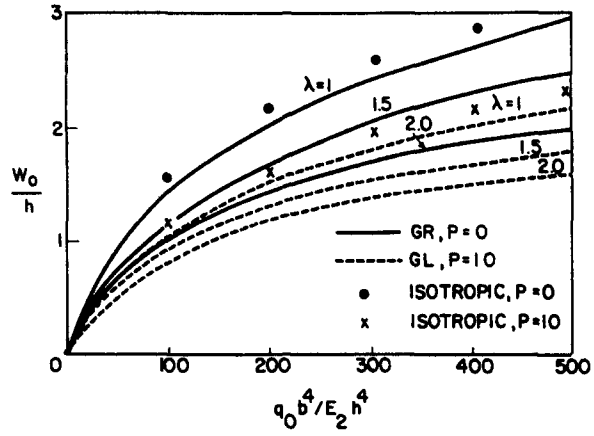

Fig. 3. Load-deflection curves for isotropic and orthotropic rectangular plates.

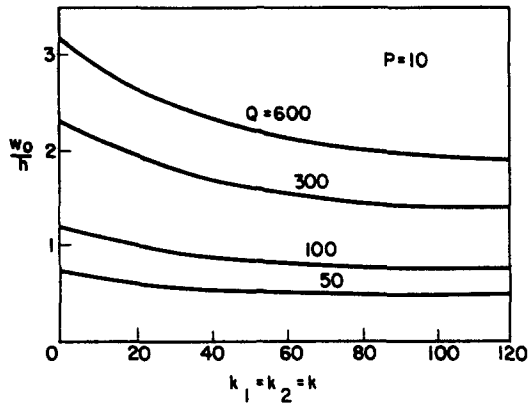

Fig. 4. Load-central deflection relation for glass-epoxy plate with uniform rotational edge restraints under uniform lateral load and in-plane tension.

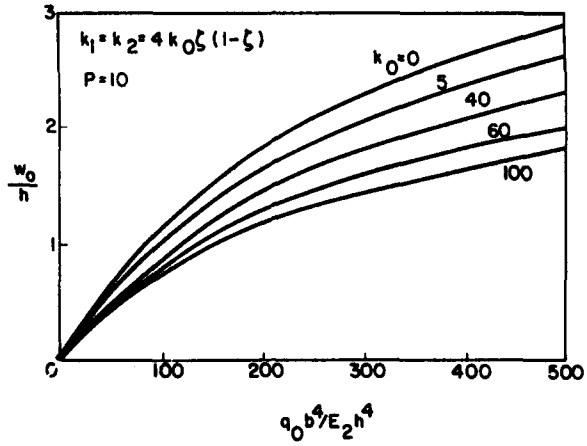

Fig. 5. Effect of non-uniform rotational edge restraint on maximum deflection of square glass-epoxy plate for various transverse loads.

($k_1 = k_2 = k$) on the central deflection of a square plate is shown in Fig. 4 for various transverse loads. It can be seen that all these curves tend to be flat for large values of k, especially for $k > 100$. This indicates that the result for these values of k is close to the clamped condition.

The load-maximum deflection relation of an orthotropic square plate under the combined action of uniform lateral load and in-plane tension, $p = 10.0$, is shown in Fig. 5

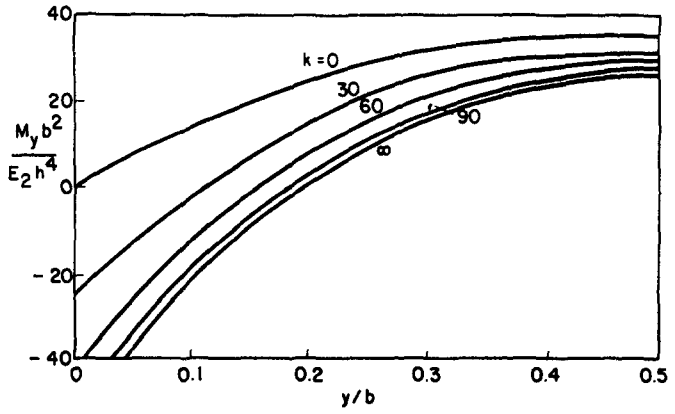

Fig. 6. Distribution of bending moment M_y along central line $x = a/2$ in uniformly loaded graphite-epoxy square plate for different rotational edge restraints ($q_o b^4/E_2 h^4 = 300$, $k_1 = k_2 = k$).

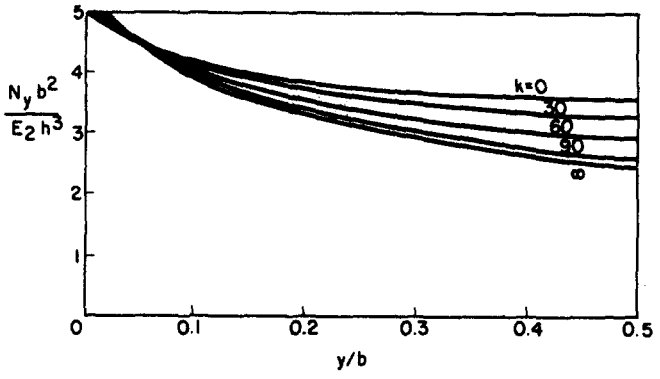

Fig. 7. Distribution of membrane force along central line $x = a/2$ in uniformly loaded glass-epoxy plate for different rotational edge restraints ($q_o b^4/E_2 h^4 = 200$, $P = 5$, $k_1 = k_2 = k$).

for various values of the rotational edge-restraint coefficient. These coefficients along the edges, $\eta = 0, 1$, are taken to be a parabolic function of ζ as

$$k_1(\zeta) = k_2(\zeta) = 4k_0(\zeta - \zeta^2)$$

where k_0 is a nondimensional constant. In this case the maximum deflection occurs on the midpoints of the unloaded edges. The value, $k_0 = 0$, corresponds to the edges, $\eta = 0, 1$, simply supported.

Figure 6 presents the bending-moment distribution along the central line $\zeta = 0.5$ in a plate for different values of the uniform rotational edge restraint. For $k < 30$ the maximum bending moment occurs at the plate center. When the value of k is gradually increased, the maximum bending moment will shift to the middle of the supported edges. The value, $k = \infty$, corresponds to the clamped edge. The distribution of the membrane force N_y along the central line $\zeta = 0.5$ in a glass-epoxy square plate under a combination of uniform load and in-plane tension is plotted in Fig. 7 for various values of uniform rotational restraint of the two loaded edges. It is observed that the membrane force changes slowly with the rotational edge restraint.

CONCLUSION

A generalized Fourier series solution for large deflections of rectilinearly orthotropic rectangular plates in the sense of von Kármán is formulated for two opposite free edges and the other edges nonuniformly and elastically restrained against rotation. These series for the deflection and stress function can be numerically shown to converge

rapidly. Numerical results for maximum deflection, bending moment and in-plane force of orthotropic plates under lateral load and in-plane tension are presented for unidirectional glass-epoxy and graphite-epoxy materials, different aspect ratios and various edge conditions. In the linear case the present result for central deflection and bending moment agrees well with available data.

Acknowledgement—The results presented in this paper were obtained in the course of research sponsored by the Natural Sciences and Engineering Research Council of Canada.

REFERENCES

1. C. Y. Chia, *Nonlinear Analysis of Plates*. McGraw-Hill, New York (1980).
2. M. Stippes, Large deflections of rectangular plates. *Proc. 1st U.S. Nat. Cong. Appl. Mech.*, pp. 339–345 (1951).
3. J. Ramachandran, Large amplitude vibration of circular plates with mixed boundary conditions. *Comput. Structures* **4**, 871–877 (1974).
4. J. L. Nowinski, Some static and dynamic problems concerning nonlinear behavior of plates and shallow shells with discontinuous boundary conditions. *Int. J. Non-Linear Mech.* **10**, 1–14 (1975).
5. M. M. Banerjee, Note on the large deflection of circular plates supported at several points along the boundary. *Bull. Cal. Math. Soc.* **68**, 279–284 (1976).
6. W. E. Alzheimer and R. T. Davis, Nonlinear unsymmetrical bending of an annular plate. *ASME J. Appl. Mech.* **35**, 190–192 (1968).
7. J. T. Tielking, Asymmetric bending of annular plates. *Int. J. Solids Structures* **16**, 361–373 (1980).
8. M. K. Huang and H. D. Conway, Bending of a uniformly loaded rectangular plate with two adjacent edges clamped and the others either simply supported or free. *ASME J. Appl. Mech.* **19**, 451–460 (1952).
9. H. J. Fletcher and C. J. Thorne, Bending of thin rectangular plates. *Proc. 2nd U.S. Nat. Cong. Appl. Mech.*, pp. 389–406 (1954).
10. S. Timoshenko and S. Woinowsky-Krierger, *Theory of Plates and Shells*. McGraw-Hill, New York (1959).
11. L. M. Keer and B. Stahl, Eigenvalue problems of rectangular plates with mixed edge conditions. *ASME J. Appl. Mech.* **39**, 513–520 (1972).
12. A. W. Leissa, P. A. A. Laura and R. H. Gutierrez, Vibrations of rectangular plates with nonuniform elastic edge supports. *ASME J. Appl. Mech.* **27**, 891–895 (1980).
13. Y. Narita, Applications of a series-type method to vibration of orthotropic rectangular plates with mixed boundary conditions. *J. Sound Vib.* **77**, 345–355 (1981).
14. Y. Narita and A. W. Leissa, Flexural vibrations of free circular plates elastically constrained along parts of the edge. *Int. J. Solids Structures* **17**, 83–92 (1981).